

Experimental evaluation of collapse deformation behavior of a rockfill material

A.A. Heshmati^{1,*}, A.R. Tabibnejad², H. Salehzadeh³, S. Hashemi Tabatabaei⁴

Received: January 2014, Revised: June 2014, Accepted: February 2015

Abstract

To investigate the saturation induced collapse deformation behavior of rockfill material, a set of large-scale triaxial tests were conducted in saturated and dry-saturated conditions. Specimens were tested under various confining pressures. For dry-saturated tests, specimens were sheared in various stress levels. Results of all dry saturated tests indicate a sudden reduction in the specimen volume during the submerging process. The ratio of the minimum axial strength of a submerged specimen (at the end of the saturation process) to the shear strength of the specimen before saturation is defined as the coefficient of stress recovery, C_{sr} . Results show that this ratio increases as the confining pressure increases, and decreases as the shear stress level increases. According to the results of dry-saturated tests, reduction values of the internal friction angle caused by saturation ($\Delta\phi_c$), the ratio of the elasticity modulus of the material after saturation to its elasticity modulus in dry condition, i.e., E_{wet}/E_{dry} , and the saturation induced sudden volumetric strain (ε_{vc}) decrease as the confining pressures increase. However the shear stress level does not have any meaningful effect on the variation of $\Delta\phi_c$, E_{wet}/E_{dry} and (ε_{vc}).

Keywords: large-scale triaxial test, rockfill material, collapse deformation, confining pressure, shear stress level, strength and deformability parameters.

1. Introduction

The extensive application of rockfill material in geotechnical structures, especially in rockfill dams during recent decades makes it inevitable to identify various behavioral aspects of these materials. Rockfill material, as with other coarse grained material undergo rapid or sudden settlements that could show relatively large values without the need of changes to the applied loads, and only due to the submerging in water [1, 2, 3, 4].

This phenomenon is called collapse deformation [3, 5, 6], and can occur due to the intensification of particle breakage and crack propagation, particle rearrangement, and facilitation of particle displacement due to the lubrication effects of water [7, 8, 9]. Saturation induced rapid settlements measured in different rockfill dams and rockfill embankments such as railway embankments [3, 5, 10] are main examples of collapse deformation.

Collapse deformation is mainly caused by heavy rains, and is frequently reported during the first impounding of the reservoir in the upstream shell of rockfill dams and other rockfill structures [11, 12, 13].

Although valuable investigations have been conducted to recognize the principles and mechanisms of collapse deformation, certain aspects of this phenomenon are still unknown.

The testing of prototype rockfill materials is near impossible because of the particles' large sizes, therefore, grain sizes are usually scaled down for laboratory testing. Due to the coarse nature of scaled material large scale laboratory tests, such as the triaxial, direct shear and odometer tests have been employed for the study of rockfill material behavior [14, 15, 16, 17, 18]. The number of these studies however, have been limited because large scale laboratory tests are expensive and difficult to perform.

An appropriate approach to an acceptable estimation of the value of collapse deformation of rockfill materials is to develop a precise numerical modeling of this phenomenon [19, 20]. Along these lines, an evaluation of the effects of stress conditions, including confining pressures and shear stress levels, on the pattern and intensity of the saturation-induced deformations can be useful.

The aim of this study is to evaluate the effects of confining pressures and shear stress levels on the collapse settlement behavior of rockfill materials during saturation. This study also seeks to identify various changes that

* Corresponding author: heshmati@iust.ac.ir

1 Assistant professor, School of Civil Engineering, Iran University of Science and Technology

2 Ph.D. Student, School of Civil Engineering, Iran University of Science and Technology

3 Assistant professor, School of Civil Engineering, Iran University of Science and Technology

4 Assistant professor, Department of Geotechnical Engineering, Road, Housing & Urban Development Research Center

affect strength and deformability parameters of rockfill materials caused by submerging. Through the uses of large scale triaxial equipment tests were conducted on both saturated and dry-saturated samples. During the dry-saturated tests (that model the first impounding of dry-constructed rockfill dams) specimens were first sheared in dry conditions up to a specified shear stress level, then the axial loading was stopped, and the specimens were gradually submerged in de-aired water. The axial loading process then continued until the failure stage. Three confining pressures and three shear stress levels were applied. In the end, results of the tests were analyzed and interpreted to explore the effects of these factors on collapse deformation behavior of rockfill materials.

2. Experimental Program

2.1. Apparatus

A large-scale triaxial apparatus with a sample diameter of 300 mm (height of 600 mm) was used for testing. The samples were sheared and strain-controlled. One LVDT sensor outside the triaxial cell and two sensors inside the cell were used to measure the vertical displacement of the samples. Vertical load was measured by means of two sensors, one inside and the other outside the cell.

2.2. Material

In this study rockfill materials were obtained from the shell borrow area of Gotvand dam, constructed on the Karun River in Iran's province of Khuzestan. Characteristics of the material, along with the standards employed for their determination, are presented in table 1.

Photos of testing material have been separated according to individual sieve sizes illustrated in Fig 1.

Table 1 Rockfill Material Characteristics

Mineralogy	Shape	Water Absorption	Gs	Los Angeles Abrasion (500 cycles)
Limestone	Subrounded to Subangular	1% ASTM (C127-128)	2.7 ASTM (C127-128)	28% ASTM (C131)

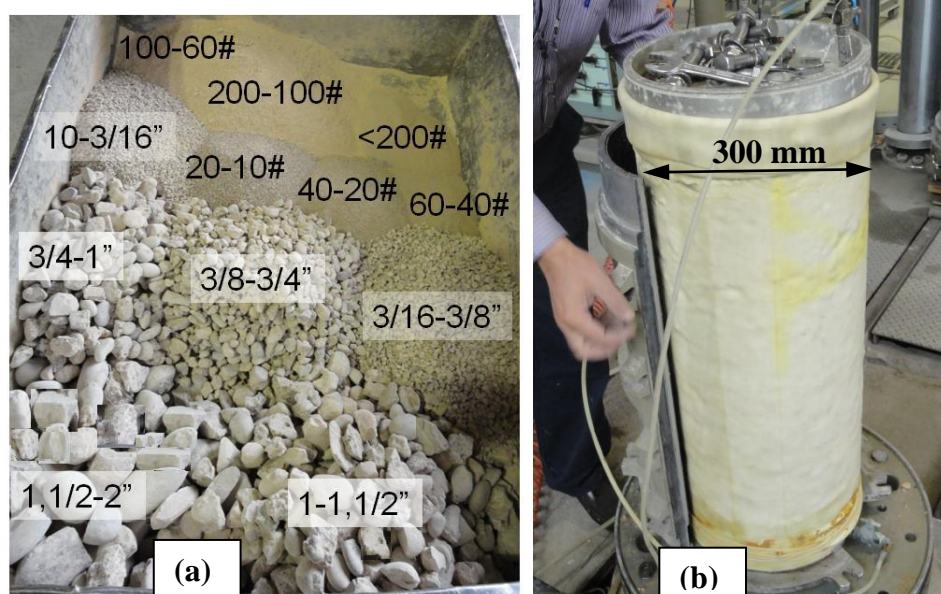


Fig. 1 (a) Testing material separated based on individual sieve size (b) prepared specimen

The prototype rockfill material had a maximum particle size of 700 mm. It is obvious that testing the prototype material was almost impossible because of its coarseness and the limitations of the triaxial cell dimensions. Therefore, the material particle sizes for laboratory test specimens were scaled down by some

degrees. According to 300mm diameter of the test samples, the maximum particle size of 2 inches (about 51 mm) was selected for testing material by using $D/d=6$. The gradation curve of testing material was $C_u=60$ and $C_c=5.9$, shown in Fig 2 along with middle (average) grain size distribution curve of the field (prototype) material.

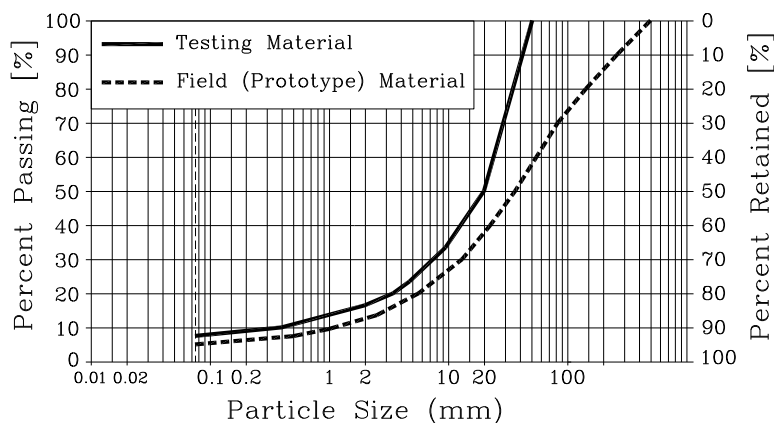


Fig. 2 Grain size distribution curves of testing material and prototype material

2.3. Testing procedure

In order to prepare specimens at the specified dry density of $\gamma_d=21.5 \text{ kN/m}^3$ and the above-mentioned gradation (Fig. 2), the quantities of various sizes of the materials were determined by weight. The individual fractions were mixed thoroughly in order to achieve a more homogenous sample.

The produced material was compacted in six layers (according to the ASTM D7181 proposed "tamping method") to achieve the required density. The strain-controlled axial loading of the specimens was applied with a rate of 1mm/min. Because of the relatively high permeability of the tested material this rate was selected based on the method proposed by ASTM D7181.

The experimental program consists of twelve large scale (300 mm in diameter) strain-controlled triaxial tests that were conducted in three confining pressures of 100, 500 and 1000 kPa. In each confining pressure four

specimens were tested, one was saturated before shearing, and the other three were first sheared (in dry conditions) up to a specified shear stress level. The axial loading (monotonic movement of the top cap) was then stopped as the specimen was gradually and fully submerged from bottom to the top under very low head of de-aired water, and resumed thereafter.

Shear stress level (SSL) is defined as the ratio of shear stress at the moment of saturation to the maximum shear strength of the specimen in dry condition. In order to evaluate the effect of SSL on the collapse settlement behavior of the material in dry-saturated tests, for each confining pressure three shear stress levels (SSL) of 0.4, 0.7 and 1.0 were specified at which the axial loading was stopped and the specimens were submerged. Table 2 shows the experimental program of this study.

In order to verify the reproducibility and repeatability of the results the dry-saturated tests with confining pressures of 500 (submerged in SSL=0.4) and 1000 kPa (submerged in SSL=0.7) were repeated.

Table 2 Experimental program

Specimen Diameter (mm)	Dry density (kN/m^3)	Confining Pressure (kPa)	Shear stress level (at the moment of saturation)	Test Name
300	21.5	100	0 (initially saturated)	100S
			0.4	100D0.4S
			0.7	100D0.7S
			1.0	100D1.0S
		500	0 (initially saturated)	500S
			0.4	500D0.4S
			0.7	500D0.7S
			1.0	500D1.0S
		1000	0 (initially saturated)	1000S
			0.4	1000D0.4S
			0.7	1000D0.7S
			1.0	1000D1.0S

3. Results

Figs. 3, 4 and 5 present the axial stress-axial strain and the volumetric strain-axial strain behavior of the tests conducted at confining pressures of 100, 500 and 1000 kPa respectively. In these figures the first number (three to four digits) represents the confining pressure value in kPa; “d” stands for the dry condition; “s” refers to saturated condition; and the number between d and s represents the shear stress level in which the specimen was submerged. In these figures the dilation is considered positive.

For each confining pressure, a dry saturated test under a shear stress level (SSL) of 1.0 was performed initially to identify the maximum shear strength of the material (in dry condition). Then the other dry-saturated tests were conducted under shear stress levels of 0.4 and 0.7; i.e. specimens were submerged in 40% and 70% of the identified maximum dry shear strength. In order to compare behavior of the dry-saturated tests with those from the saturated tests, in each confining pressure one test was carried out on an initially saturated specimen.

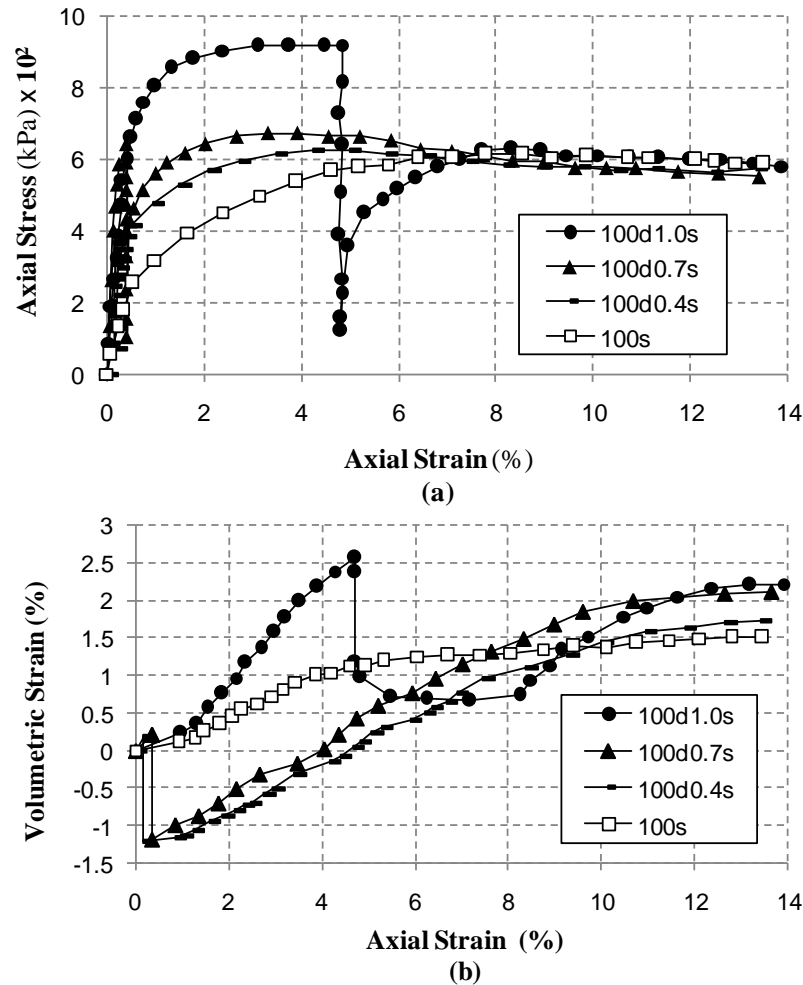
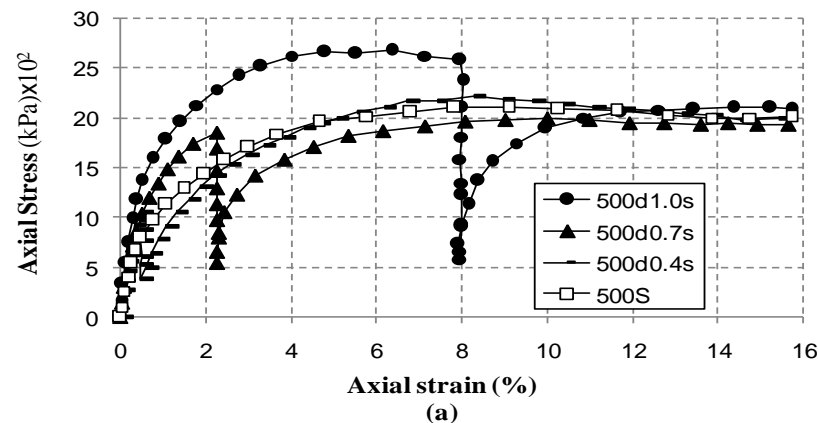


Fig. 3 a) Axial stress-axial strain b) volumetric strain-axial strain behavior of tests conducted at confining pressures of 100 kPa



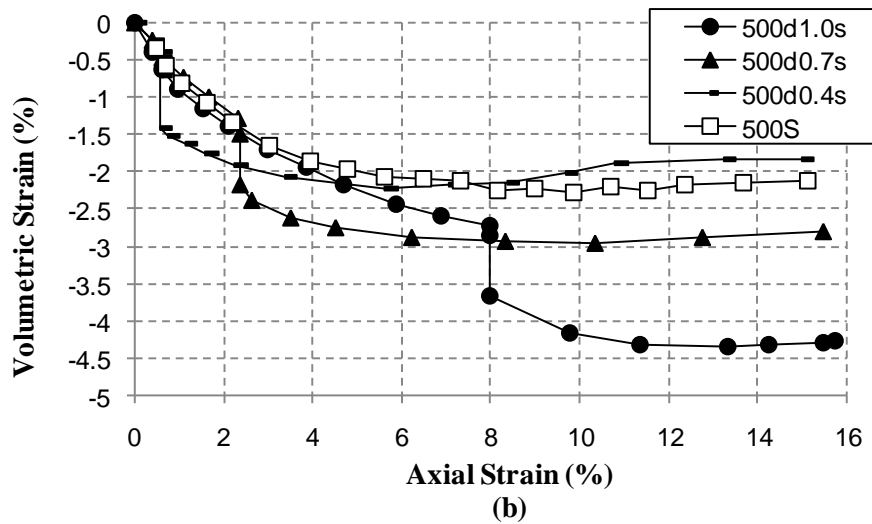


Fig. 4 a) Axial stress-axial strain b) volumetric strain-axial strain behavior of tests conducted in confining pressure of 500 kPa

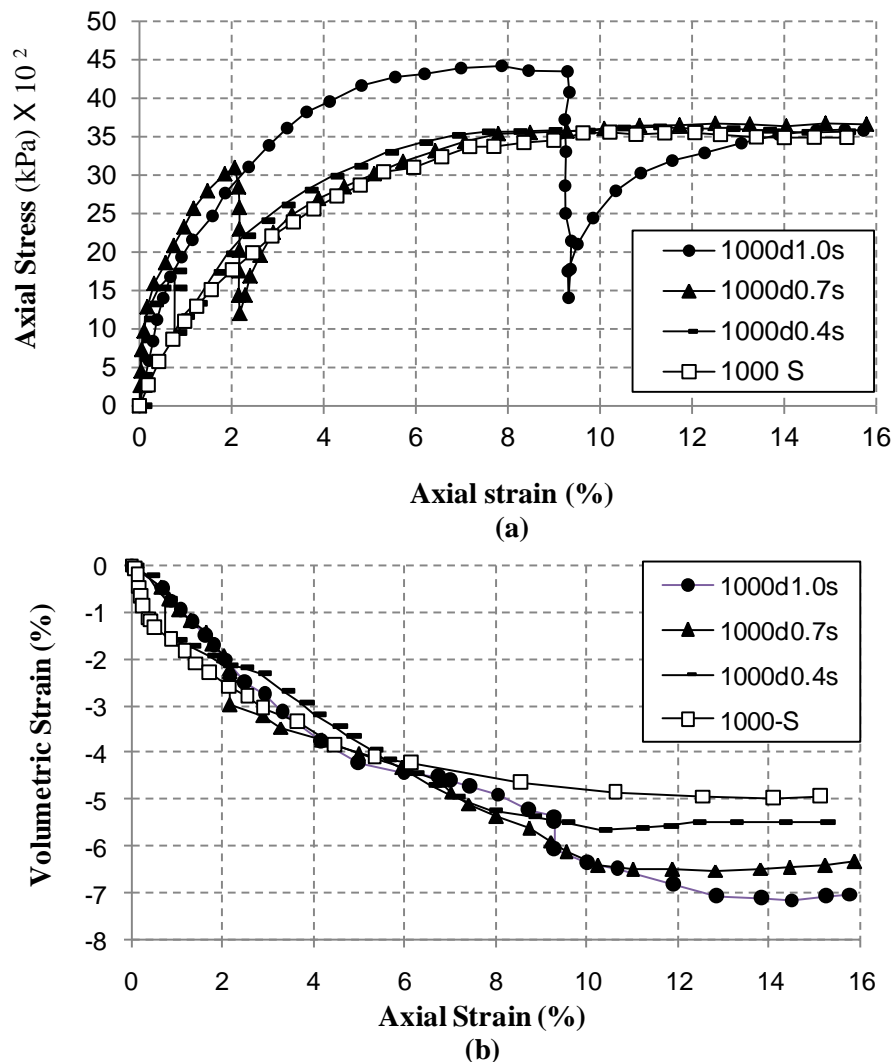


Fig. 5 a) Axial stress-axial strain b) volumetric strain-axial strain behavior of tests conducted in confining pressure of 1000 kPa

According to Figs. 3 to 5, a sudden reduction of axial stress (representing shear strength of the specimens) was observed in a constant axial strain due to saturation in all of the dry-saturated tests. Given the existing literature, these behaviors were expected. However one of the goals

of this study was to estimate the value of this reduction and to find out its dependence (if any) to the confining pressure and SSL (in the moment of saturation). When the specimens were completely submerged with de-aired water, the axial stress had reached its minimum value and

remained constant, then the monotonic movement of the top cap restarted and the axial stress increased to a maximum value and stayed approximately constant to the end of the test. Results of the final shear strength of the submerged specimens were very close to the maximum strength of the initially saturated specimens, tested under the same confining pressures.

4. Analysis of the Results

The ratio of the minimum axial strength (deviatoric stress) of a submerged specimen (at the end of the saturation process) to the shear strength of the specimen before saturation is defined as the coefficient of stress recovery, C_{sr} . Fig 6 illustrates the equation,

$$C_{sr} = \frac{\sigma_{d2}}{\sigma_{d1}} \quad (1)$$

Where σ_{d1} and σ_{d2} represent the deviatoric stresses before saturation and at the end of saturation process, respectively.

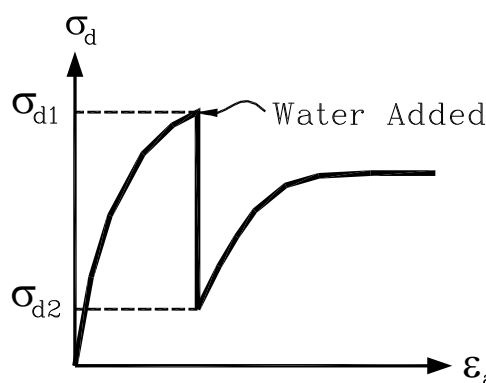


Fig. 6 Typical behavior of dry-saturated specimens

Through the application of Equation (1), values of C_{sr} were calculated for all dry-saturated tests. Fig. 7 presents the variation of C_{sr} versus confining pressure for the three shear stress levels.

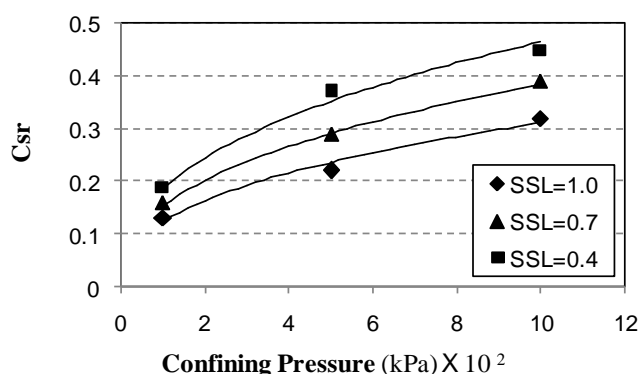


Fig. 7 Coefficient of stress recovery (C_{sr}) versus confining pressure for dry-saturated tests

As illustrated in Fig. 7, an increase in confining pressures leads to an increase in the coefficient of stress

recovery (C_{sr}). Under specified confining pressures, C_{sr} decreases as the shear stress level (SSL) increases. According to this figure, for each value of SSL a trendline is drawn for the $C_{sr} - \sigma_3$ data, and an equation with the following general form could be suggested for each.

$$C_{sr} = m \left(\frac{\sigma_3}{P_a} \right)^\alpha \quad (2)$$

Where σ_3 is the confining pressure, P_a represents the atmospheric pressure. Results show the obtained value of coefficient α to be 0.4.

The calculated values of coefficient m in Equation (2) for shear stress levels of 0.4, 0.7 and 1 are 0.185, 0.153 and 0.124, respectively. Fig. 8 illustrates the variation of coefficient m against shear stress levels.

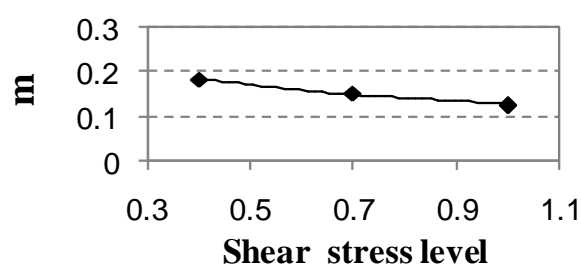


Fig. 8 Coefficient m versus shear stress level for dry-saturated tests

The following equation could be suggested for m -SSL data.

$$m = \beta (SSL)^{-\alpha} \quad (3)$$

Results show the obtained value of coefficient β to be 0.13. If coefficient m from Equation (3) was to be substituted in Equation (2), the following equation could be presented for estimating the coefficient of stress recovery, C_{sr} .

$$C_{sr} = \beta \left(\frac{\sigma_3}{SSL \cdot P_a} \right)^\alpha \quad (4)$$

The aforementioned equation has been obtained and proven valid for purposes of this study, and may not be applicable for testing other types of rockfill materials and stress conditions.

While results of Equation 4 have also been obtained for material and stress range purposes of this particular study, obtaining and using the C_{sr} coefficient can nonetheless be an appropriate approach for the estimation of post saturation shear stresses, as in a numerical analysis to specify the values of shear stresses in the elements one cycle after submerging.

The tests to determine the axial stress-axial strain and the volumetric strain-axial strain curves were repeated twice so to prove the accuracy of the results as shown in Fig 9(a) and 9(b), respectively.

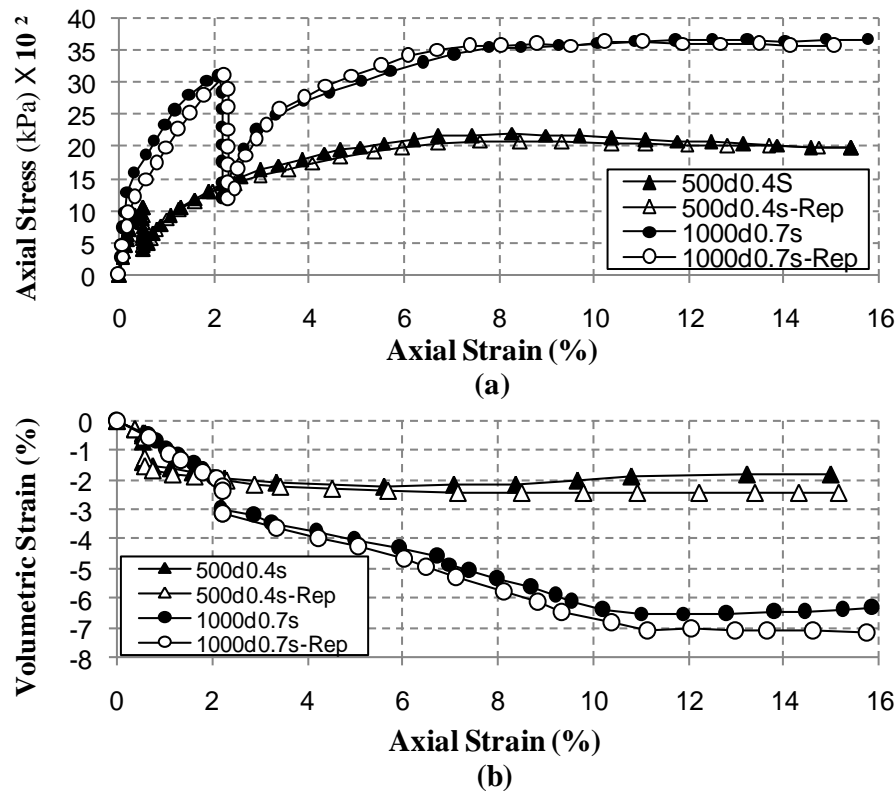


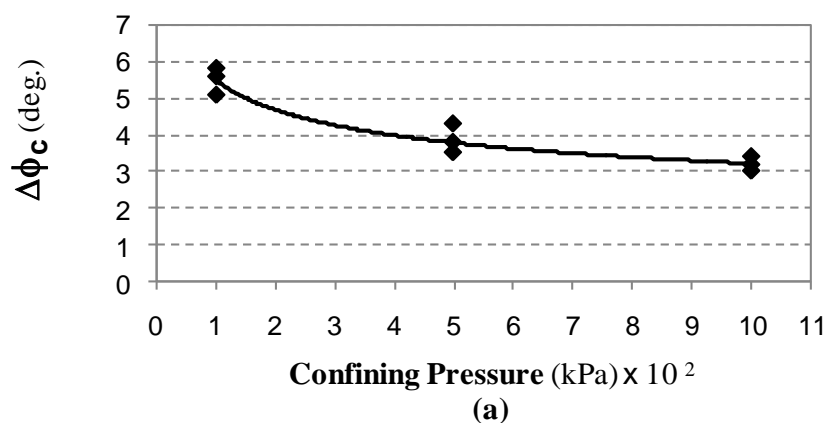
Fig. 9 a) Axial stress-axial strain b) volumetric strain-axial strain behavior of repeated dry-saturated tests under confining pressures of 500 and 1000 kPa, and submerged in SSL of 0.4 and 0.7

4.2. Internal friction angle

According to the literature, saturation degrades the strength parameters of rockfill materials [1, 4, 21]. Results of the dry-saturated tests were analyzed to probe the effects of confining pressures and shear stress levels (at the moment of saturation) on the intensity of this degradation.

Values of the maximum principal stresses σ_1 were obtained from dry conditions (before saturation), see Figs. 3(a) to 5(a). After obtaining the submerged maximum

shear strength, the values of σ_1 could be specified for the specimens saturated in different shear stress levels. In order to calculate reduction values of the internal friction angle ($\Delta\phi_c$) caused by saturation, values of shear stress levels and internal friction angles for each confining pressure were obtained under both dry and saturated conditions. Variations of the reductions (values of $\Delta\phi_c$) versus the confining pressures and SSL are illustrated in Figs. 10(a) and 10(b), respectively.



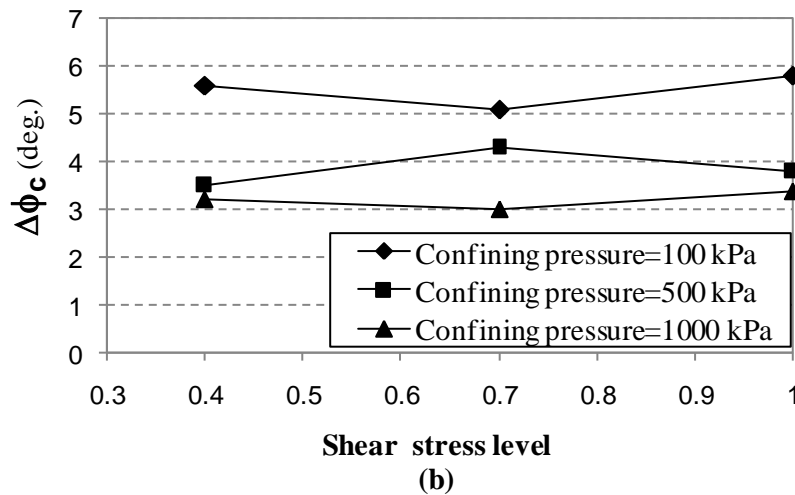


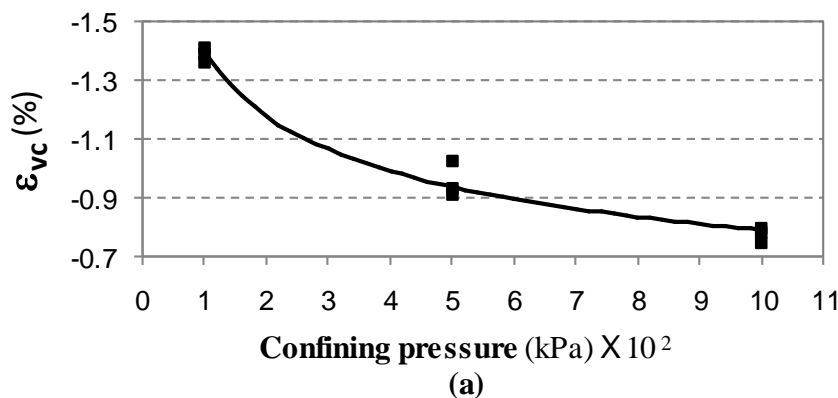
Fig. 10 Reduction of internal friction angle due to saturation ($\Delta\phi_c$), a) versus confining pressure, b) versus shear stress level

These figures indicate that the value of $\Delta\phi_c$ (reduction of the internal friction angle caused by saturation) decreases as the confining pressure increases. It should be noted that coarse material, and in particular rockfill, has a nonlinear failure envelope and the internal friction angle of these materials, even in dry condition, decreases by increasing confining pressure [23, 24]. Reduction in the dilation angle of the material due to breakage of sharp contact edges of the particles (reduction of the particles surfaces roughness) in higher values of confining pressure may be responsible for this nonlinearity of rockfill failure envelope [25]. Therefore as confining pressures increase in dry conditions, a larger portion of the mentioned events that cause internal friction angle to degrade take place before submerging. As a result, when material is submerged in higher confining pressures, and the internal friction angle caused by saturation ($\Delta\phi_c$) is decreased as the confining pressure is increased, fewer events (i.e. particle edge breakages) are left behind to occur during the saturation process. However, there is no clear trend for variation of $\Delta\phi_c$ against SSL. The shear stress level (at the moment of saturation) does not have any meaningful effect on the variation of $\Delta\phi_c$.

4.3. Deformation behavior and parameters

Turning to Figs. 3(b) to 5(b) it can be seen that in comparatively low confining pressures of 100 kPa, due to relatively high dry density of the specimens, dilation governs the deformation behavior of the material. Also, a general trend of volume increase (positive values of volumetric strain) was observed during deviatoric loading. An increase of confining pressures to higher values (i.e. 500 and 1000 kPa) brings about a decrease in the volume of the specimens during deviatoric loading, which evidently makes the dilation effect inconsiderable.

What can be seen in Figs. 3(b) to 5(b) is a sudden reduction in the volume of the specimens during the submerging process as observed for all of the dry-saturated tests (in a constant axial strain). This observation is compatible with the saturation-induced sudden settlements reported in the literature for oedometer or direct shear tests on rockfill materials [1, 2, 26, 27]. Values of these sudden reductions in volumetric strain (ε_{vc}) are plotted against a confining pressure and shear stress level (SSL, at the moment of saturation) (Fig. 11(a) and 11(b)).



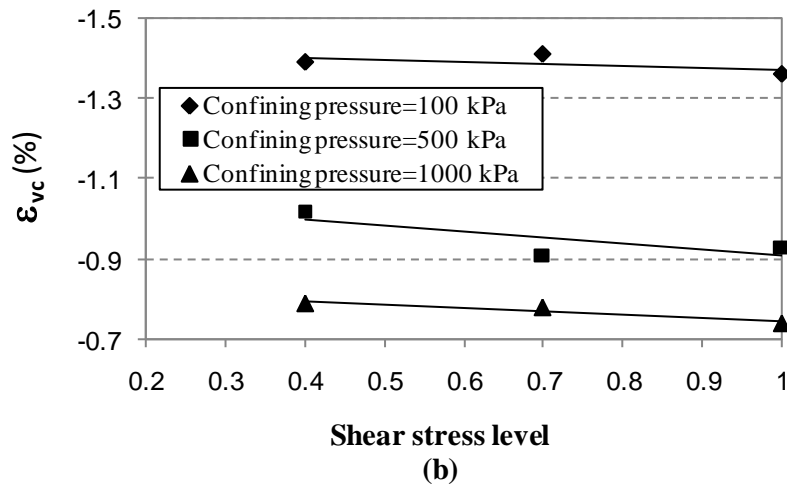


Fig. 11 Change in volumetric strain due to saturation (ϵ_{vc}), a) versus confining pressure, b) versus shear stress level.

These figures show that the saturation-induced sudden volumetric strain (ϵ_{vc}) decreases (in absolute value) as the confining pressure increases. According to Figs. 3(b) to 5(b), by increasing the confining pressure, higher values of volumetric strain occur under dry conditions, and the material becomes denser and more compressed before submerging. An increase in the confining pressure can lead

to less deformation during saturation of the material. However, the shear stress level does not have considerable effect on the variation of ϵ_{vc} .

Table 3 illustrates the changes present in the deformation parameters of the materials due to saturation, elasticity modulus of the specimens under dry conditions, and submerging.

Table 3 Elasticity modulus of the material in dry and saturated conditions

Test Name	Confining Pressure (kPa)	Shear stress level (at the moment of saturation)	Elasticity modulus in dry condition E_{dry} (mPa)	Elasticity modulus after submerging E_{wet} (mPa)	E_{wet}/E_{dry}
100S	100	0 (initially saturated)	250	60	0.24
100D0.4S		0.4		65	0.26
100D0.7S		0.7		55	0.22
100D1.0S		1.0		55	0.22
500S	500	0 (initially saturated)	700	120	0.17
500D0.4S		0.4		115	0.16
500D0.7S		0.7		125	0.18
500D1.0S		1.0		120	0.17
1000S	1000	0 (initially saturated)	1200	165	0.14
1000D0.4S		0.4		155	0.13
1000D0.7S		0.7		175	0.15
1000D1.0S		1.0		175	0.15

In dry-saturated tests, the elasticity modulus of the specimens in dry condition (E_{dry}) is obtained by drawing a tangent line to the first part (before saturation) of the axial stress-axial strain (σ_a - ϵ_a) curve. The elasticity modulus of the material after submerging (E_{wet}) is obtained by drawing a tangent line to the reloading part (after completion of the submerging process) of the σ_a - ϵ_a curve. Fig 12 shows the

tests performed under confining pressures of 500 kPa.

The ratio of the elasticity modulus of the material after saturation to their elasticity modulus in dry condition, *i.e.*, (E_{wet}/E_{dry}), are cited in Table 2. The variations of this ratio (E_{wet}/E_{dry}) versus confining pressures and shear stress levels (SSL, at the moment of saturation) are presented in Figs. 13(a) and 13(b), respectively.

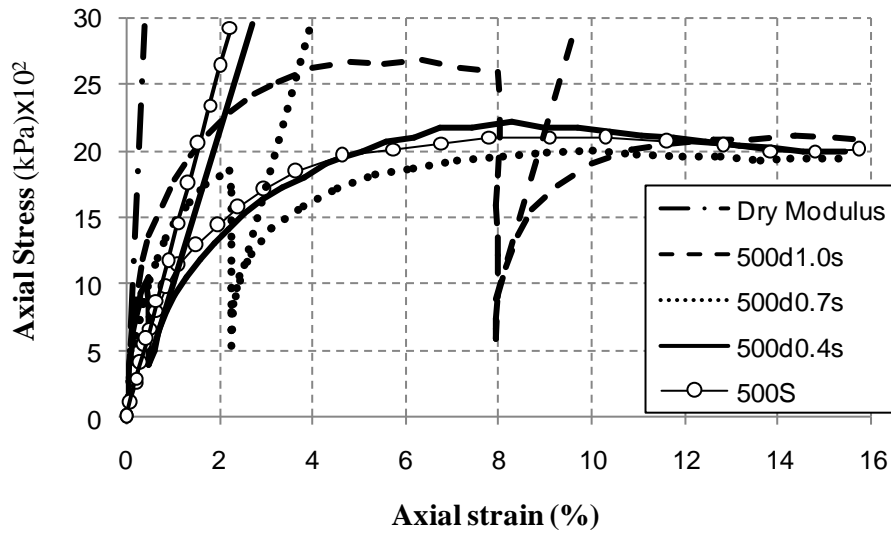


Fig. 12 Prior and post-saturation elasticity modulus of the material from dry-saturated tests

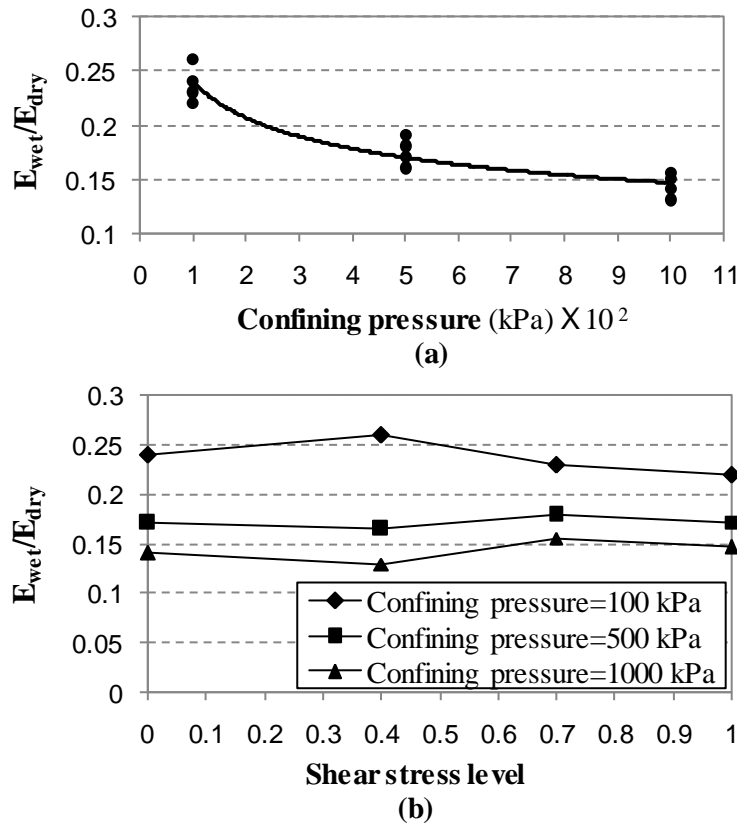


Fig. 13 Ratio of the material elasticity modulus under saturated condition to the elasticity modulus under dry condition (E_{wet}/E_{dry}), a) versus confining pressure, b) versus shear stress level

These figures show that the ratio of E_{wet}/E_{dry} decreases as the confining pressure increases. However, the values of this ratio remain unaffected by the shear stress level, and there is no clear trend for the variation of this ratio (E_{wet}/E_{dry}) against SSL.

5. Discussion

5.1. Verification of the results

As mentioned before, in the literature, the studies that

have investigated the collapse deformation behavior of rockfill materials by means of large-scale tests are limited. It is obvious that in these studies, due to differences in the mineralogy, dry density, gradation curves and etc. of the testing materials, the results will not match in values. However, the general variation trends may be comparable.

In order to verify the validity of the results presented in this study, the variation trends of C_{sr} , $\Delta\phi_c$, and E_{wet}/E_{dry} against confining pressures were compared to that of other available investigations. Since the maximum dry shear strength of the materials in other investigations have not

been specified, therefore it was not possible to determine the shear stress level at which the specimens were submerged. Hence, a comparison between the variation trends and shear stress levels could not be made.

Figs. 14 to 16 illustrate, respectively, the variations of

C_{sr} , $\Delta\phi_c$ and E_{wet}/E_{dry} against confining pressures, obtained from this study and other investigations [26, 27, 28]. In these figures “T” stands for triaxial test and “DS” refers to direct shear test.

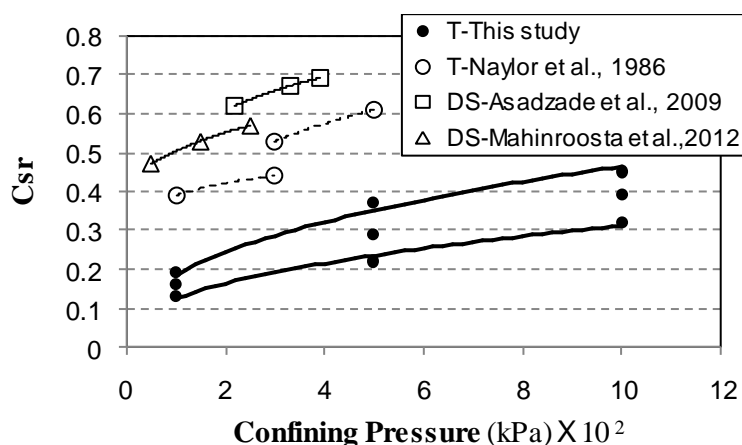


Fig. 14 Comparison of C_{sr} variations against confining pressures, obtained from this study and other investigations

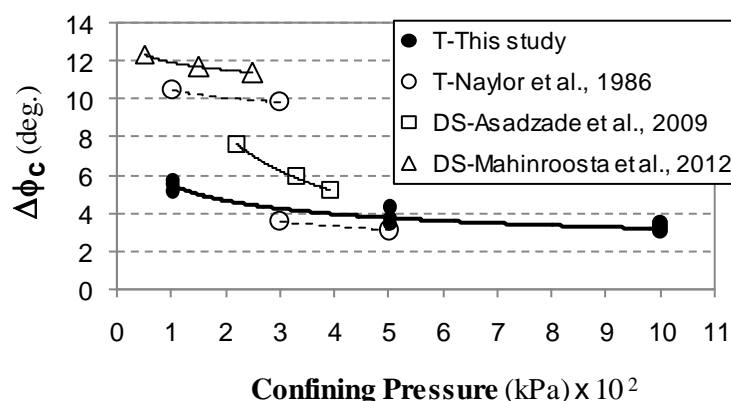


Fig. 15 Comparison of the variation of $\Delta\phi_c$ against confining pressures, obtained from this study and other investigations

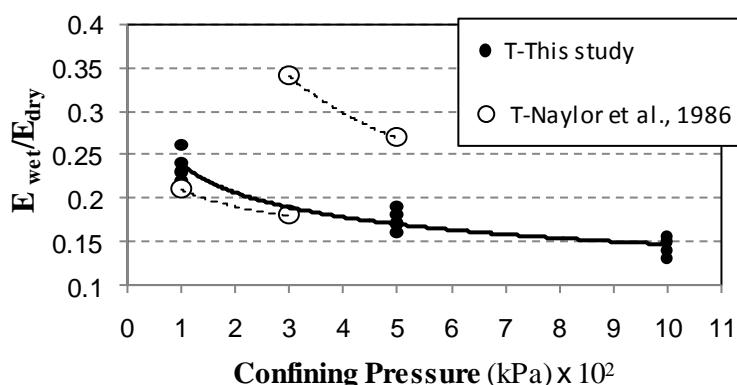


Fig. 16 Comparison of the variation of E_{wet}/E_{dry} against confining pressures, obtained from this study and another investigations

It should be mentioned that in the case of the direct shear test, because of the directions of loading and applied displacement and according to the boundary conditions, the confining pressures differ at various points inside the specimen. In this study it was assumed that in the direct shear test, an at-rest condition is applicable and a K_0 coefficient of 0.5 was considered. Therefore, an estimation

of the specimens' mean confining pressure was made by multiplying the normal stress by $K_0 (=0.5)$.

Since the stress paths and the directions of the applied loads and displacements in the direct shear and triaxial tests are different, it was not possible to compare the variations of E_{wet}/E_{dry} against confining pressures in the two types of tests. Hence this comparison was limited to

the results of the triaxial tests. The triaxial tests that their results were compared to results of this study included two sets of tests that had been conducted on two different rockfill materials. The differences in the results of the two sets of tests are most probably due to different mineralogy and strength of the mentioned materials [27].

According to Figs. 14 to 16, the general variation trends of C_{sr} , $\Delta\phi_c$ and E_{wet}/E_{dry} against confining pressures obtained from other investigations are compatible with results obtained from this study. However, differences in the mineralogy, dry density and gradations of the testing materials all contribute to the different results. Other factors that also contribute to different results in the direct shear tests include differences in the stress paths and boundary conditions (compared to triaxial tests).

5.2. Particle breakage

The intensity of particle breakage of the testing materials was evaluated by the comparison of the pre-test and post-test grain-size distributions. The particle breakage is usually expressed quantitatively by the breakage index, B_g [25]. The value of B_g is obtained by sieving the testing

material by a set of sieves (50 to 0.075 mm) before and after testing. The difference in percentage of the particles retained on each sieve size is determined by Equation 5.

Where W_{ki} is the percent retained on sieve size k before the test and W_{kf} represents the percent retained on the same sieve size after the test.

Due to particle crushing, percentage of the particles retained in large size sieves will decrease, and percentage of particles retained in small size sieves will increase. The sum of decreases will be equal to the sum of increases in the retained percentages. The breakage index, B_g , is the sum of the differences in the retained percentage on sieves, only with the same sign (sum of decreases or increases). This index is expressed as a percentage in Equation 6.

$$B_g = \sum_k \Delta W_k \quad (6)$$

In this study values of the particle breakage index, B_g , is calculated for all tests. Plots of this index against confining pressures and shear stress levels are presented in Figs. 17a and 17b, respectively.

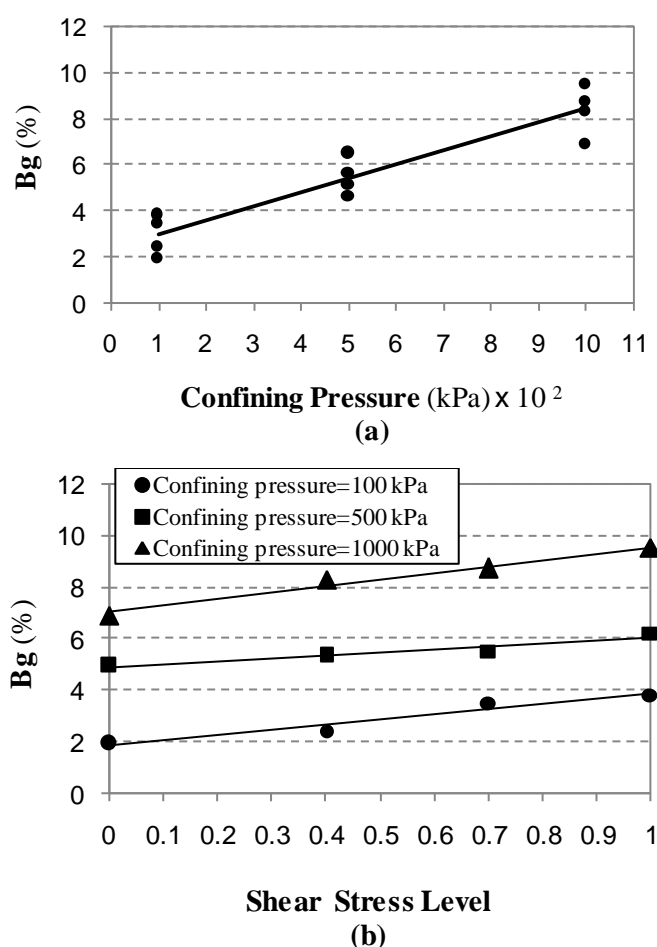


Fig. 17 Particle breakage index, B_g , a) versus confining pressure, b) versus shear stress level.

Fig. 17a indicates that the value of particle breakage index, B_g , increases almost linearly by increasing the confining pressure. This observation is compatible with

the trends reported in the literature [26, 29, 30, 31, 32].

Fig. 17b illustrates a slight increase in the particle breakage index, B_g , as the shear stress level (at the

moment of submerging) increases. For each confining pressure, the initially saturated specimen ($SSL=0$) shows the lowest value of B_g . The easier sliding of particles in the initially saturated tests may strongly have been due to the lubrication effect of water, which may have been responsible for the comparatively lower particle breakages. The specimens that were submerged at higher shear stress levels experienced higher values of shear stresses and shear strains under dry conditions (without the lubrication effect of water) and therefore, exhibited higher values of B_g .

6. Summary and Conclusions

A set of large-scale triaxial tests was conducted to investigate the saturation-induced collapse settlement behavior of a rockfill material. Specimens were tested in saturated and dry-saturated conditions at three confining pressures. For dry-saturated tests, specimens were submerged in three shear stress levels. Effects of the confining pressure and shear stress level (at the moment of saturation) on the collapse deformation behavior of rockfill material were explored and the changes in the strength and deformability parameters of rockfill material caused by submerging were evaluated.

Result comparisons for the tests performed in both saturated and dry-saturated conditions indicated that under a certain confining pressure, the final maximum shear strengths of submerged specimens, independent of the shear stress level at the moment of saturation, are very close to each other, such that they are approximately equal to that of initially saturated specimens.

The ratio of the minimum axial strength (deviatoric stress) of a submerged specimen (at the end of the saturation process) to the shear strength of the specimen before saturation is defined as the coefficient of stress recovery, C_{sr} . Results of dry-saturated tests has shown that this ratio increases as the confining pressure increases, and decreases as the shear stress level (SSL at the moment of saturation) increases. Based on these results an equation was suggested to estimate the value of C_{sr} . Even though this equation was formulated for the material and stress range purposes of this particular study, nevertheless, solving and using the C_{sr} coefficient could be an appropriate approach to estimating the post saturation shear stresses, *e.g.* in a numerical analysis to specify the values of shear stresses in the elements one cycle after submerging.

Based on the results, saturation degrades the strength and deformability parameters of rockfill material. Results of dry-saturated tests evidenced that the values of internal friction angle reduction caused by saturation ($\Delta\phi_c$) decreases as the confining pressure increases; however, the shear stress level (at the moment of saturation) does not have any meaningful effect on the variation of $\Delta\phi_c$.

The results indicated that the ratios of the elasticity modulus of the material after saturation to their elasticity modulus in dry conditions, *i.e.*, (E_{wet}/E_{dry}), decrease with a non-linear trend as confining pressures increase; however, the values of this ratio are not affected by the shear stress

levels and there is no clear trend for variation of this ratio (E_{wet}/E_{dry}) against SSL .

Under certain confining pressures the elasticity modulus of submerged specimens, independent of the shear stress level at the moment of saturation, are close to each other and are close to the value of elasticity modulus obtained for initially saturated specimens. This value could be considered the elasticity modulus of the material in saturated conditions (under confining pressure).

In all of the dry-saturated tests, a sudden reduction in the volume of the specimens was observed during the submerging process (in a constant axial strain). This observation is compatible with the saturation-induced sudden settlements reported in the literature for oedometer or direct shear tests on rockfill materials.

The results evidenced that the saturation induced sudden volumetric strain (ε_{vc}) decreases (in absolute value) by increasing the confining pressure; however the shear stress level has no considerable effect on the variation of ε_{vc} .

In order to verify the validity of the results presented in this study the variation trends of C_{sr} , $\Delta\phi_c$ and E_{wet}/E_{dry} against confining pressure were compared to results of other available investigations. The general variation trends of the mentioned parameters against confining pressures obtained from other investigations are compatible with results obtained from this study. However, due to the differences in the mineralogy, dry density and gradations of the testing materials the values of the results are different.

Breakage of the particles was observed during the triaxial tests. Value of particle breakage index, B_g , increases almost linearly by increasing confining pressure. In addition, B_g , slightly increases by increasing the shear stress level (at the moment of submerging).

Acknowledgments: The tests were performed at the Laboratory of the Geotechnical Department of Road, Housing & Urban Development Research Center in Tehran, Iran. The authors are grateful to Dr. A. Aghaei, Mr. H. Hasani and Mr. Sarchami (the laboratory staff) for their useful comments and assistance in conducting the tests.

References

- [1] Alonso E. Exploring the limits of unsaturated soil mechanics: The behavior of coarse granular soil and rockfill, The 11th Spencer J. Buchanan lecture, College station Hilton, Texas, T.X, 2003.
- [2] Alonso E, Oldecop LA. Fundamentals of rockfill collapse, Proceeding of the Asian Conference on Unsaturated Soils, UNSAT-ASIA, Singapore, 2000, pp. 3-13.
- [3] Alonso E, Cardoso R. Behavior of materials for earth and rockfill dams: Perspective from unsaturated soil mechanics, Proceeding of the 2nd International Conference of Long Term Behavior of Dams, Graz, Austria, 2009.
- [4] Soroush A, Aghaei Araei A. Analysis of behavior of a high rockfill dam, Proceeding of the Institution of Civil Engineering, Geotechnical engineering, 159(GEI), 2006, pp. 49-59.

- [5] Oldecop LA, Alonso E. Theoretical investigation of the time-dependent behavior of rockfill, *Geotechnique*, 2007, No. 3, Vol. 57, pp. 289-301.
- [6] Pourjafar A, Mahin roosta R. Evaluation of the collapse settlement behavior of sandy material using triaxial shear tests, *Proceeding of the 6th National Congress of Civil Engineering*, Semnan, Iran, 2011.
- [7] Soroush A, Aghaei Araei A. Uncertainties in mechanical behavior of rockfills during first impounding of rockfill dams, *Proceeding of the 73rd Annual meeting of ICLOD*, Tehan, Iran, No. 186-S5, 2005.
- [8] Silvani C, Bonelli S, Philippe P, Desoyer T. Buoyancy and local friction effects on rockfill settlement: A discrete modeling, *Journal of Computers and Mathematics with Applications*, 2008, Vol. 55, pp. 208-217.
- [9] Houston SL, Houston WN, Zapata CE, Lawrence C. Geotechnical engineering practice for collapsible soils, *Journal of Geotechnical and Geological Engineering*, 2001, Vol. 19, pp. 333-355.
- [10] Tabibnejad AR, Mahin Roosta R. Evaluation of Marun Rockfill dam behavior during the construction and operation period using instrumentation system data, *Modares Civil Engineering Journal (M.C.E.L)*, 2011, No. 1, Vol. 11, pp. 99-115.
- [11] Ohta H, Ishiguro T, Mori Y, Uchita Y, Tsuruta S, Takahashi A. Uncertainties in safety evaluation of large rockfill dams during first filling, *Proceeding of the 73rd Annual meeting of ICLOD*, Tehan, Iran, 2005, No. 082-S5.
- [12] Touileb BN, Bonelli S, Anthinac P, Carrere A, Debordes O, LA Berbera G, Bani A, Mazza G. Settlement by wetting of the upstream rockfills of large dams, *Proceeding of the 53rd Canadian Geotechnical Conference*, Montreal, 2000, pp. 263-270.
- [13] Soriano A, Sanchez FJ. Settlement of railroad high embankment, *Proceedings of the 12th European Conference on Soil Mechanics and Geotechnical Engineering*, Amsterdam, 1999, pp. 1885-1890.
- [14] Varadarajan A, Sharma K, Venkatachalam K, Gupta A. Testing and modeling two rockfill materials, *Journal of Geotechnical and Geoenvironmental Engineering*, No. 3, Vol. 129, pp. 206-218.
- [15] Indraratna B, Ionescu D, Christie HD. Shear behavior of railway ballast based on large-scale triaxial tests, *Journal of Geotechnical and Geoenvironmental Engineering*, 1998, No. 5, Vol. 124, pp. 439-449.
- [16] Aghamajidi M. Laboratory investigation of creep in rockfill Material, MSc thesis, Tarbiat Modarres University, Tehran, Iran, 2004, (in Persian).
- [17] Eshtaghi V, Mahin roosta R. Changes in the stress and strain conditions of dry gravelly material caused by saturation, *Proceedings of the 4th International Conference of Soil Mechanics and Geotechnical Engineering of Iran*, Tehran, Iran, 2010, No. & Code: 190-TVMTMAH.
- [18] Aghaei Araei A, Razeghi H, Ghalandarzadeh A, Hashemi Tabatabaei S. Effects of loading rate and initial stress state on stress-strain behavior of rock fill materials under monotonic and cyclic loading conditions, *Scientia Iranica*, 2012, No. 5, Vol. 19, pp. 1220-1235.
- [19] Naylor DJ, Maranha Das Neves E, Veiga Pinto AA. A back analysis of Beliche dam, *Geotechnique*, 1997, No. 2, Vol. 47, pp. 221-233.
- [20] Escuder I, Andreu J, Rechea M. An analysis of stress-strain behavior and wetting effects on quarried rock shells, *Canadian Geotechnical Journal*, 2005, Vol. 42, pp. 51-60.
- [21] Salehi D, Tabibnejad AR, Feizi Khankandi S. Evaluation of strength and deformability parameters of the rockfill shell material of Gotvand dam, *Proceeding of the 2nd National Conference on Dam and Hydropower (NCDH)*, Tehan, Iran, 2008, pp. 77-86.
- [22] Xu M, Song E, Chen J. A large triaxial investigation of the stress-path-dependent behavior of compacted rockfill, *Acta Geotechnica*, 2012, No. 3, Vol. 7, pp. 167-175.
- [23] Charles JA, Watts KS. The influence of confining pressure on the shear strength of compacted rockfill, *Geotechnique*, 1980, No. 4, Vol. 30, pp. 353-367.
- [24] Lowe J. Shear strength of coarse embankment dam materials, *Proceeding of the 8th International Congress on Large Dams*, 1964, pp. 745-761.
- [25] Marsal RJ. Large scale testing of rockfill materials, *Journal of the Soil Mechanics and Foundation Division*, ASCE, 1967, No. 2, Vol. 93, pp. 27-43.
- [26] Asadzadeh M, Soroush A. Direct shear testing on a rockfill material, *The Arabian Journal for Science and Engineering*, 2009, No. 2B, Vol. 34, pp. 379-396.
- [27] Naylor DJ, Maranha Das Neves E, Mattar D, Veiga Pinto AA. Prediction of construction performance of Beliche dam, *Geotechnique*, 1986, No. 3, Vol. 36, pp. 359-376.
- [28] Mahinroosta R, Oshtaghi V. Evaluation of the effects of saturation on strength and collapse settlement of coarse materials using direct shear tests, *Sharif Civil Engineering Journal*, 2011, No. 1, Vol. 29-2, pp. 103-114.
- [29] Aghaei Araei A, Soroush A, Rayhani M. Large-Scale triaxial testing and numerical modeling of rounded and angular rockfill materials, *Sientia Iranica Journal, Transaction A: Civil Engineering*, 2010, No. 3, Vol. 17, pp. 169-183.
- [30] Bazazzadeh H, Kalantary F, Asakereh A. An investigation on the effect of particle breakage on rockfill constitutive parameters, *EJGE, Bund. J*, 2011, Vol. 15, pp. 847-864.
- [31] Indraratna B, Nimbalkar S, Christie D. The performance of rail track incorporating the effects of ballast breakage, confining pressure and geosynthetic reinforcement, *8th International Conference on the Bearing Capacity of Roads, Railways, and Airfields*, London, UK, 2009, pp. 5-24.
- [32] Ghanbari A, Hamidi A, Abdolazadeh N. A study of the rockfill material behavior in large-scale tests, *Civil Engineering Infrastructures Journal*, 2013, No. 2, Vol. 46, pp. 125-143.